JACS
JOURNAL OF THE AMERICAN CHEMICAL SOCIETY
Article
pubs.acs.org/JACS

Photolysis of an Amphiphilic Assembly by Calixarene-Induced Aggregation

Yi-Xuan Wang, Ying-Ming Zhang, and Yu Liu*

Department of Chemistry, State Key Laboratory of Elemento-Organic Chemistry, Collaborative Innovation Center of Chemical Science and Engineering (Tianjin), Nankai University, Tianjin 300071, P. R. China

Supporting Information

ABSTRACT: Photosensitizers generally show great tendency for self-aggregation in aqueous media, leading to quenched fluorescence and lower photosensitizing ability. Herein, we report that amphiphilic anthracene is highly photoreactive after aggregation induced by *p*-sulfonatocalix[4]arene in water. The formation of a host−guest supramolecular assembly and the photolysis of the anthryl core are identified by UV−vis and NMR spectroscopy, dynamic light scattering, and transmission electron microscopy. Additionally, the assembly exhibited efficient photolysis with visible light in the presence of exogenous photosensitizers. This approach could be extended to various photoresponsive self-assemblies and applications in phototherapy and the design of photodegradable materials.

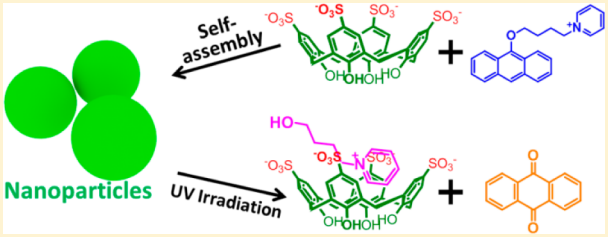

INTRODUCTION

Benefiting from cleanness, high efficiency and low cost, light has become one of the most desirable stimuli for regulating molecular structures and aggregate behaviors of molecular assemblies.[1] Superior to other external signals, light is a noninvasive stimulus that can be readily triggered from outside of the system to adequately control the physicochemical properties of multicomponent assemblies. Photoreactions can be initiated, stopped, or even paused by the reversible switching of the light's wavelength and intensity without adding any exogenous substances.[2] Consequently, photoactive molecules are widely used to construct photomodulated materials, which are used in soft lithography,[3] separation technology,[4] and photodynamic therapy.[5]

Among the various photoresponsive systems, photolyzable matrices that can irreversibly decompose after irradiation have received much attention in the design of degradable materials, drug delivery vehicles, and tissue engineering systems.[6] Supramolecular approaches are an alternative way to build photolyzable materials. Such assemblies are held together by multiple weak noncovalent interactions that can be easily tuned by external stimuli, and more importantly, the tectons are generally small molecules, which favor dissipation of the assembly.[7] Many studies have investigated the fabrication of photoresponsive supramolecular assemblies,[8] but photolytic materials with high efficiency are still needed. Among the numerous noncovalent interactions, the host−guest complexation based on macrocyclic receptors is particularly advantageous in constructing water-soluble supramolecular architectures.[9] *p*-Sulfonatocalix[n]arenes (SCnAs) are a prominent family of water-soluble calixarene derivatives with versatile inclusion/complexation properties for various types of guest molecules in aqueous media.[10] With high water solubilities and excellent biocompatibilities, SCnAs are appealing candidates for biological and pharmaceutical applications.[11] Moreover, SCnAs have a unique tendency to modulate the aggregation behavior of aromatic or amphiphilic molecules by decreasing the critical aggregation concentration, enhancing aggregate compactness, and regulating the degree of order in the aggregates, which is referred to as calixarene-induced aggregation (CIA) by our group.[12] Herein, we demonstrate a design strategy for a photolyzable assembly, based on CIA between SC4A and amphiphilic 9-alkoxy-substituted anthracene (AnPy). Anthracenes are highly reactive upon light irradiation, and the reversible anthracene dimerization is a model for photo-cross-linking of functional materials.[13] In addition, anthracene can trap singlet oxygen and form stable endoperoxides, which is useful for the detection of singlet oxygen.[14] However, application in the development of photolyzable assemblies has not been fully explored.[15] In this work, we fabricated a photolyzable supramolecular assembly, employing SC4A as the host and AnPy as the photoactive guest (Scheme 1). SC4A not only induced compact packing between anthracenes but also inhibited the fluorescence quenching of AnPy, which is favorable for photosensitization. Interestingly, the photodecomposition of aggregated AnPy was significantly promoted, while it was reported that the fluorescence of photosensitizers could be generally self-quenched after aggregation,[16] resulting in greatly reduced ability for singlet oxygen generation and lower photoreactivity.[17] The supramolecular assembly exhibited efficient photolysis with visible light in the presence of exogenous photosensitizers. To the best of our knowledge,

Received: February 11, 2015
Published: March 24, 2015

DOI: 10.1021/jacs.5b01566
J. Am. Chem. Soc. 2015, 137, 4543−4549

Scheme 1. Schematic Illustration of the Photolyzable Supramolecular Amphiphilic Assembly

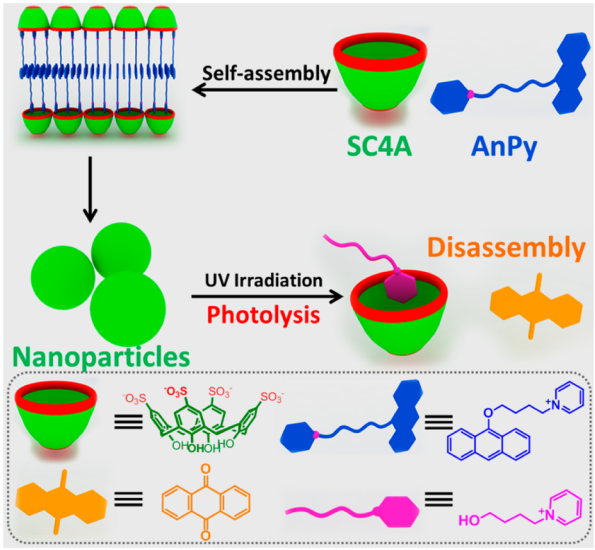

such a photolyzable system promoted by supramolecular aggregation has not been reported to date.

RESULTS AND DISCUSSION

Construction and Characterization of the Amphiphilic Supramolecular Assembly. SCnAs are thought to greatly reduce electrostatic repulsion in the cationic head groups of the amphiphilic guests and facilitate guest aggregation via host–guest complexation. Therefore, the high binding affinities between the SCnAs and the cationic head groups of the guests are crucial for high-performance CIA.[12a] The binding constant (K_a) between AnPy and SC4A was determined by the fluorescence spectral titration. As shown in Figure 1, the

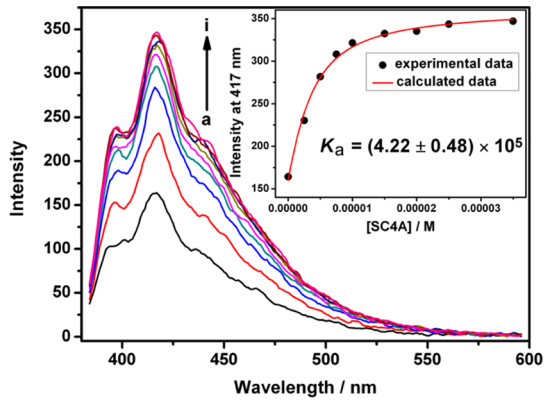

Figure 1. Alterations of the fluorescence spectra of AnPy (5.0 μM) upon addition of SC4A (0–35 μM, from (a) to (i)) in aqueous solution at 25 °C. Inset: the nonlinear least-squares analysis of the variation of fluorescence intensity with the concentration of SC4A to calculate the binding constant (λ_{ex} = 365 nm and λ_{em} = 417 nm).

emission intensity of AnPy at 417 nm gradually increased upon addition of SC4A. Furthermore, a peak was reached at a molar fraction of 0.5 in the Job plot, indicating the 1:1 binding stoichiometry between SC4A and AnPy (Figure S3, Supporting Information). After validating the complex stoichiometry, the K_a value could be calculated as 4.22 × 10^5 M^{-1} using a nonlinear least-squares curve-fitting method by analyzing the sequential changes in the fluorescence intensity of AnPy in the presence of varying concentrations of SC4A. The enhanced fluorescence of the SC4A–AnPy complex may be ascribable to a regulated intramolecular photoinduced electron transfer (PET) process.[18] For free AnPy, the PET process takes place from the anthracene moiety as an electron-rich donor to the pyridinium moiety as an electron-deficient acceptor. After complexation with SC4A, the pyridinium moiety was included in the electron-rich cavity of SC4A, and therefore the nonradiative channel in the PET process was spontaneously inhibited to a great extent, leading to an enhanced emission intensity of the anthracene fluorophore.

Similar to many other amphiphilic molecules reported before, AnPy could be induced by SC4A to form large assemblies via host–guest interaction. The critical aggregation concentration of AnPy in the presence of SC4A was measured by monitoring the dependence of the optical transmittance at 600 nm on the concentration of AnPy. In the absence of SC4A, the optical transmittance of AnPy at 600 nm showed no appreciable change as the concentration increased from 0.01 to 0.20 mM (Figure S4, Supporting Information). However, upon addition of SC4A, the optical transmittance decreased gradually as the concentration of AnPy increased because of the formation of the large amphiphilic assembly. According to the plot of optical transmittance at 600 nm versus the concentration of AnPy, the calixarene-induced critical aggregation concentration was obtained as ca. 0.06–0.10 mM (Figures 2a and S5, Supporting Information). There is no tendency for SC4A to self-aggregate in aqueous solution.[19] To determine the optimal molar ratio of the intermolecular aggregation between SC4A and AnPy, the optical transmittance of AnPy at a fixed concentration (0.10 mM) was monitored while increasing the concentration of SC4A. As shown in Figures 2b and S6 (Supporting Information), the transmittance at 600 nm first gradually decreased until reaching a minimum at an SC4A/AnPy ratio of 0.4 and then increased upon further addition of SC4A. The decrease in the left-hand portion of inflection is due to the formation of a higher-order complex of SC4A with AnPy, further resulting in a supramolecular amphiphilic assembly. However, the assembly converted into simple inclusion complexes upon addition of excess SC4A. The strong electrostatic repulsion among the complexes prevents them from nanoaggregation, eventually leading to an increase in the optical transmittance. Therefore, the optimal mixing ratio for the amphiphilic assembly was SC4A:AnPy = 2:5. A clear shoulder absorption band at ca. 408 nm was observed in the UV–vis absorption spectrum of the SC4A–AnPy assembly, which is attributed to aggregation of anthracene moieties (Figure S7a, Supporting Information).[20] However, this absorption band was not observed for free AnPy, even at high concentrations (Figure S7b, Supporting Information), or the aggregates formed by similar 9-substituted amphiphilic anthracene.[21] The intrinsic electrostatic repulsion between the pyridinium moieties is unfavorable for the π–π stacking between the anthracene rings of AnPy, whereas the anthracene rings can stack with each other more tightly once the pyridinium head in AnPy is surrounded by the cavity of the negatively charged SC4A through electrostatic attraction. A control experiment showed that no assembly appeared when replacing SC4A with its fragment 4-phenolsulfonic sodium under comparable conditions (Figure S7, Supporting Information), indicating that the cyclic tetramer structure of SC4A is

DOI: 10.1021/jacs.5b01566
J. Am. Chem. Soc. 2015, 137, 4543–4549

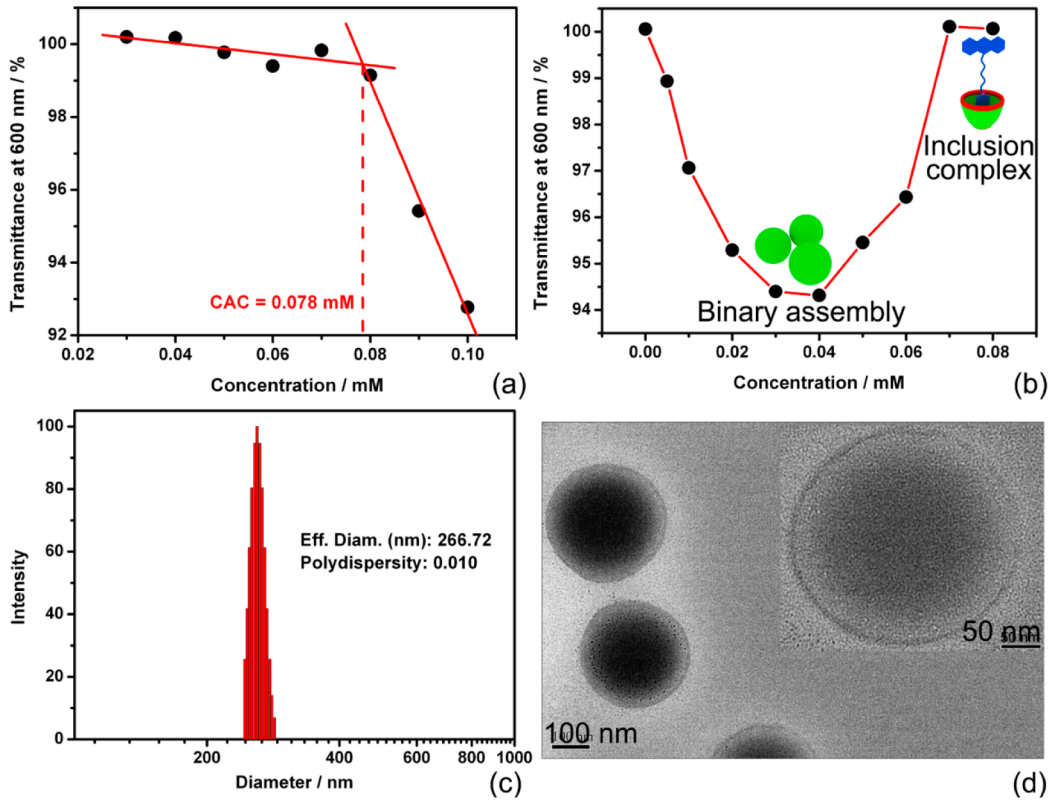

Figure 2. (a) Dependence of the optical transmittance at 600 nm on the AnPy concentration (0.03−0.10 mM) in the presence of SC4A (0.05 mM) in water at 25 °C. (b) Dependence of the optical transmittance at 600 nm on the SC4A concentration (0−0.08 mM) with a fixed AnPy concentration (0.10 mM) in water at 25 °C. Inset: Schematic illustration of the SC4A−AnPy assembly and the corresponding simple inclusion complex. (c) DLS data of the SC4A−AnPy assembly at 25 °C. (d) TEM images of the SC4A−AnPy assembly. Inset: magnified TEM image.

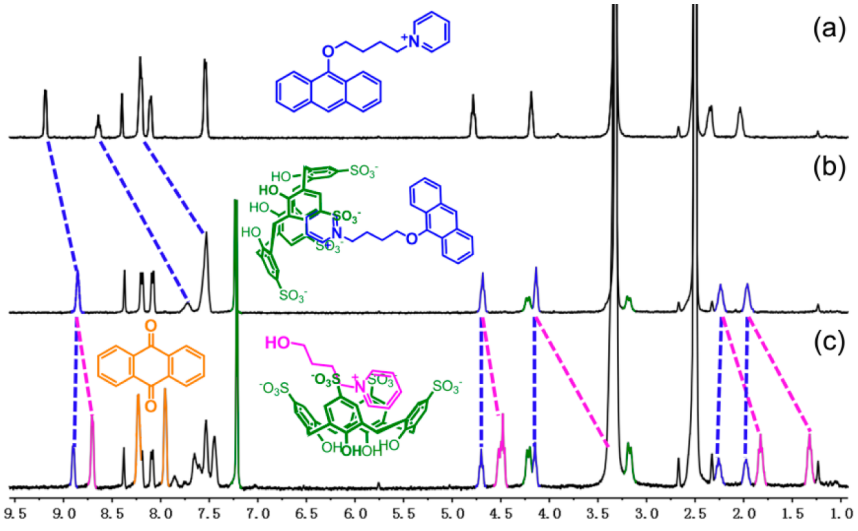

Figure 3. ^{1}H NMR spectra of AnPy in the (a) absence and (b) presence of SC4A, and (c) the SC4A−AnPy assembly after UV irradiation (365 nm) in DMSO-d_6 for 30 min ([SC4A] = 0.96 mM and [AnPy] = 2.4 mM). The peaks of unreacted AnPy, 1-(4-hydroxybutyl)pyridinium, anthraquinone, and SC4A are denoted in blue, pink, orange, and green, respectively.

undoubtedly the critical factor in inducing the supramolecular amphiphilic assembly.

Subsequently, dynamic light scattering (DLS) and transmission electron microscopy (TEM) were employed to identify the morphology and size distribution of the SC4A−AnPy assembly. As shown in Figure 2c, SC4A−AnPy assemblies exhibit a narrow size distribution with an average hydrodynamic diameter of 266.72 nm at a scattering angle of 90°. Free AnPy cannot form any aggregates under comparable conditions (Figure S8, Supporting Information), suggesting that the complexation of SC4A with AnPy can induce the critical decrease in aggregation concentration of amphiphilic AnPy. Moreover, spherical nanoparticles with diameters ranging from 200 to 400 nm were observed in the TEM images, indicative of the formation of the supramolecular aggregation in the SC4A−AnPy system (Figure 2d). Meanwhile, the particles were found

DOI: 10.1021/jacs.5b01566
J. Am. Chem. Soc. 2015, 137, 4543−4549

to possess negative ζ potential, primarily due to the residual negative charges on SC4A upon complexation with pyridinium-bearing AnPy (Figure S9, Supporting Information).

NMR spectroscopy is a powerful tool to determine complex structures. We performed ^{1}H NMR measurements in DMSO-d_6 instead of D_2O because undesirable intermolecular aggregation drastically broadens the signals, making them unidentifiable. As shown in Figure 3a,b, the proton signals of pyridinium exhibited pronounced upfield shifts owing to the ring current effect of the aromatic nuclei of calixarene,[22] while those of the anthracene rings were not appreciably affected. These results demonstrate that the pyridinium moieties are encapsulated in the calixarene cavity, while the anthracene moieties remain outside. This molecular binding behavior supports the claim that the intramolecular PET process in AnPy is inhibited by complexation with SC4A, as validated by the fluorescence titration experiments. Combining all the aforementioned results, a plausible mechanism for SC4A−AnPy assembling is deduced as illustrated in Scheme 1, where the anthryl rings anchored by the SC4A−pyridinium complexation are tightly packed to each other by the hydrophobic and $\pi-\pi$ interactions and the partly deprotonated phenol groups at the lower rim of SC4A are exposed to the aqueous solution.[23]

Thermoresponsiveness and Photolysis of the Supramolecular Assembly. The thermoresponsive assembly/disassembly processes are considered as one of the basic properties in noncovalently linked system. Because the complexation of SC4As with organic cations and the $\pi-\pi$ stacking of anthracenes are both dominantly enthalpy-driven processes, the equilibrium speciation could shift toward the enthalpically unfavorable partners upon heating.[24] Therefore, the SC4A−AnPy assembly is expected to respond to temperature. As shown in Figure S10a (Supporting Information), the scattering intensity of the solution decreased gradually with temperature increases from 25 to 40 °C and reached a plateau upon further increase in temperature, which reflects disassembly. More powerful evidence comes from the optical transmittance measurements (Figure S10b, Supporting Information). After warming the assembly solution at 40 °C for several minutes, the optical transmittance at long wavelengths increased to approximately 100%, suggesting that the SC4A−AnPy assembly completely disappeared. The reversible assembly/disassembly process was easily repeated by simply adjusting the temperature (Figure 4).

Upon excitation by UV irradiation, it was known that anthracene could be capable of being directly excited and prone to react with singlet oxygen to form stable cyclic endoperoxides.[25] However, for 9-alkoxy-substituted anthracenes, the rearrangement and further oxidation of their endoperoxides lead to the formation of anthraquinone and relevant alkanols (Scheme S1, Supporting Information).[26] Accordingly, UV−vis absorption measurements were performed to monitor the decomposition of AnPy. As shown in Figure S7a (Supporting Information), the absorption of the anthracene moiety in the range of 300−400 nm slightly decreased after irradiation by UV light at 365 nm for 30 min, implying that only a small amount of AnPy had decomposed. Comparatively, the absorption of the anthracene moiety in the SC4A−AnPy assembly decreased significantly after UV irradiation with accompanying formation of precipitates, which clearly implies that the photodecomposition of AnPy is significantly enhanced after aggregation with SC4A. Light irradiation at 365 nm cannot influence the structural change of SC4A because SC4A alone shows no

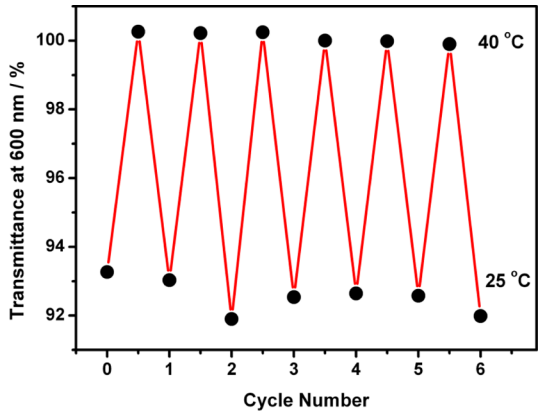

Figure 4. Optical transmittance changes of the SC4A−AnPy assembly at 600 nm over several cycles of thermal equilibration in water at 25 and 40 °C.

appreciable absorption above 300 nm.[27] This photochemical phenomenon is quite interesting because the aggregation of photosensitizers always leads to a severe self-quenching of the excited state, accompanied by a quenched fluorescence intensity and reduced capability for singlet oxygen generation.[28] To investigate the mechanism for this CIA-promoted photodecomposition, we first identified the photolytic products by mass spectrometry (MS) and ^{1}H NMR. After UV irradiation at 365 nm for 30 min, the sample of the SC4A−AnPy assembly was lyophilized and then redissolved in DMSO-d_6 for ^{1}H NMR measurements. Despite a residue of unreacted AnPy, peaks corresponding to the pyridinium and alkyl chain of AnPy were split into two groups, and new peaks at 8.71, 4.48, 3.37, 1.83, and 1.32 ppm could be assigned to the 1-(4-hydroxybutyl)-pyridinium product after irradiation (Figures 3c and S11c, Supporting Information). The signal at 4.52 ppm that disappeared upon addition of D_2O could be assigned to the proton of the hydroxyl group (Figure S11, Supporting Information). The m/z peak of 1-(4-hydroxybutyl)pyridinium at 152.1 was also observed in the ESI-MS spectrum (Figure S12, Supporting Information). The precipitate product was separated by filtration and confirmed as anthraquinone by EI-MS and ^{1}H NMR measurements (Figure S13, Supporting Information). Combining all of the aforementioned results, we can deduce that the AnPy in SC4A−AnPy assembly decomposed into 1-(4-hydroxybutyl)pyridinium and anthraquinone, as illustrated in Scheme S1 (Supporting Information).

The photodecomposition rates of AnPy and the SC4A−AnPy assembly were further examined by UV−vis spectroscopy. For free AnPy, photodecomposition proceeded very slowly, and <20% of AnPy decomposed upon irradiation at 365 nm for 60 min (Figure 5a). Additionally, the photodecomposition process at low AnPy concentrations (<0.10 mM) remained unchanged but was gradually reduced as a function of increasing AnPy concentrations (>0.10 mM). Irradiation was performed under air, and the concentration of oxygen in aqueous solution is ca. 0.28 mM, which can limit further oxidation at high AnPy concentrations. For the SC4A−AnPy assembly, 52% of AnPy decomposed after irradiation at 365 nm for only 15 min, indicating that the photodecomposition rate of AnPy was significantly enhanced in the presence of SC4A (Figure 5b). After inletting argon for 10 min at room temperature, photodecomposition proceeded more slowly. However, an increased photodecomposition rate was observed

DOI: 10.1021/jacs.5b01566
J. Am. Chem. Soc. 2015, 137, 4543−4549

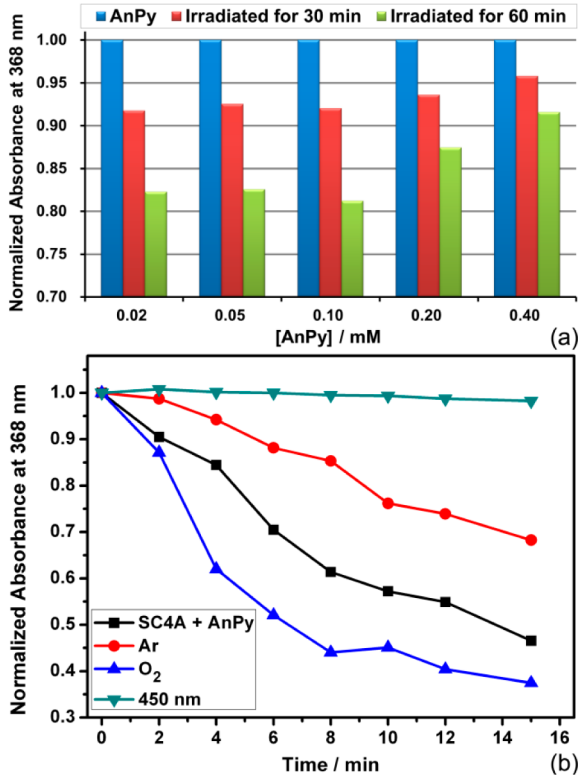

Figure 5. Normalized absorbance of (a) AnPy (measured at 25 °C) and (b) the SC4A–AnPy assembly (measured at 40 °C) at 368 nm upon irradiation for different amounts of time.

when using oxygen instead of argon. Control experiments showed no decrease in the absorption of AnPy when irradiating the solution at 450 nm under comparable conditions, suggesting that the photosensitization of anthracene is crucial to the decomposition reaction (Figure 5b). Because AnPy decomposes into insoluble anthraquinone and hydrophilic alkanol, the SC4A–AnPy assembly is expected to dissipate after irradiation. Indeed, DLS measurements gave a wide size distribution (polydispersity: 0.548) with a large hydrodynamic diameter (up to 1.3 μm) for the irradiated assemblies, and the signal for the SC4A–AnPy assembly disappeared after irradiation, corresponding to disassembly and precipitation (Figure S14a, Supporting Information). Moreover, spherical morphologies were not observed in the TEM image after irradiation (Figure S14b, Supporting Information). Taken together, these results suggest that the SC4A–AnPy assembly photodissipated successfully.

The mechanisms of this CIA-promoted photodecomposition were investigated by fluorescence spectrometry. The emission intensity of the SC4A–AnPy assembly was comparable to free AnPy, suggesting that the included AnPy retained its photosensitivity with no quenched fluorescence upon aggregation (Figure S15a, Supporting Information). Even though a relatively higher emission intensity of AnPy was observed when the supramolecular assembly was transferred into the simple SC4A–AnPy inclusion complex in the presence of excess SC4A, the inclusion complex showed a similar decomposition rate to that of free AnPy (Figure S15, Supporting Information). Therefore, we assume that the photolysis enhancement is possibly due to (i) the increased solubility of oxygen and/or the elongated lifetime of singlet oxygen in the hydrophobic assembly core than in bulk water;[29] and (ii) the closely packed anthryl rings in the SC4A–AnPy assembly facilitate communication with singlet oxygen to further self-oxidization, because the efficacy of photosensitization relies on the proximity of sensitizers and their targets.[30]

Finally, we further examined the photolysis of the SC4A–AnPy assembly upon irradiation with visible light. Eosin Y, a commonly used generator for singlet oxygen after exposure to green light, was chosen as the auxiliary photosensitizer. The absorption of eosin was broadened in the presence of AnPy or the SC4A–AnPy assembly, possibly due to the $\pi-\pi$ stacking between eosin and anthracene (Figure 6a).[15] DLS data further

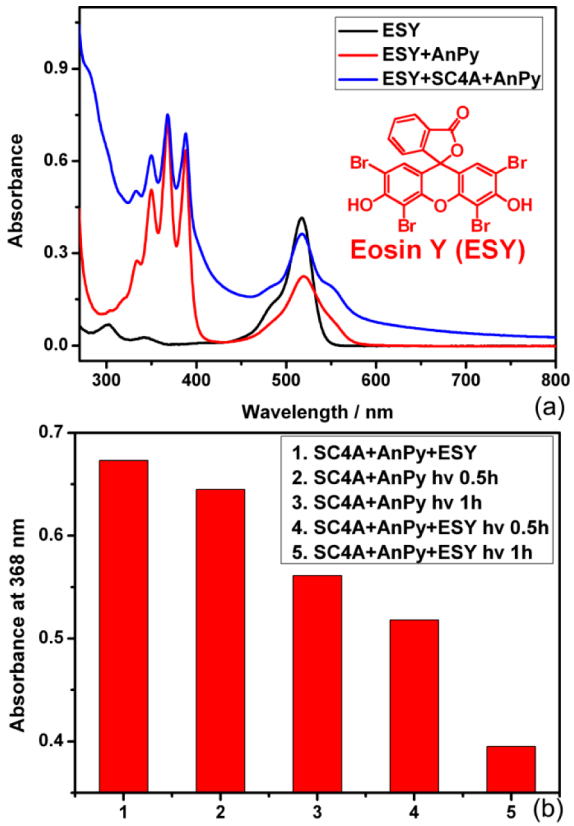

Figure 6. (a) UV–vis absorption spectra of eosin (0.01 mM), eosin with AnPy (0.10 mM), and eosin with the SC4A–AnPy assembly in water at 25 °C (with 1% ethanol). (b) Absorbance of the SC4A–AnPy assembly at 368 nm in the absence and presence of eosin upon irradiation at 520 nm for different amounts of time (measured at 40 °C).

show that no obvious size change occurs in the presence of eosin, indicating that the introduction of eosin at such a low concentration does not make any negative effect on the structural stability of binary assembly (Figure S16, Supporting Information). Upon irradiation at 520 nm, the supramolecular assembly exhibited higher efficiency in photodecomposition than free AnPy (Figure 6b), confirming that the AnPy-involved photolytic process was greatly accelerated by exogenous singlet oxygen.

CONCLUSIONS

We constructed a supramolecular photolyzable assembly based on the host–guest complexation between a macrocyclic receptor SC4A and a photodecomposable guest AnPy. The obtained nanoparticles possessed a narrow distribution and

DOI: 10.1021/jacs.5b01566
J. Am. Chem. Soc. 2015, 137, 4543–4549

could be reversibly modulated by temperature change. Upon UV light irradiation, AnPy slowly decomposed into anthraquinone and alkanol, but its photodecomposition rate was remarkably promoted after aggregation with SC4A, accompanied by the dissipation of the binary amphiphilic assembly. Moreover, the SC4A−AnPy assembly exhibited efficient photolysis with visible light in the presence of eosin Y as an exogenous photosensitizer. This approach can be used to construct various photoresponsive self-assembled materials, thus making CIA a promising strategy in the fields of photodynamic therapy and the photodegradation of pollutants.

EXPERIMENTAL SECTION

Materials. Anthrone (Aladdin), 1,4-dibromo butane (Aladdin), 4-phenolsulfonic sodium (Acros Organics), and eosin Y (Sigma-Aldrich) were used without further purification. SC4A was synthesized and purified according to procedures reported previously.[31] The storage solution of SC4A (1 mM) was adjusted to pH 7.2 using aqueous NaOH (1 M), and the pH value for the SC4A−AnPy assembly was 6.3, which is consistent with that of free AnPy. Such a slightly acidic environment could facilitate the decomposition of 9-anthryl ether. The mixing concentration for the amphiphilic assembly was 0.04 mM for SC4A and 0.10 mM for AnPy throughout the work, unless mentioned otherwise.

Synthesis. *9-(4-Bromobutoxy)anthracene.* A mixture of anthrone (2.0 g, 10.3 mmol), 1,4-dibromo butane (9.0 g, 41.7 mmol) and K_2CO_3 (14.0 g, 101.3 mmol) in 120 mL of acetone was heated to reflux for 14 h under an argon atmosphere. After cooling to room temperature, the solvent was removed via rotary evaporation under reduced pressure, and the resulting residue was purified by column chromatography (CH_2Cl_2:petroleum ether = 1:10) to yield 9-(4-bromobutoxy)anthracene (1.77 g, 52%) as a white powder. ^{1}H NMR (400 MHz, $CDCl_3$): δ 8.31−8.18 (m, 3H), 8.07−7.95 (m, 2H), 7.55−7.40 (m, 4H), 4.23 (t, 2H), 3.62 (t, 2H), 2.38−2.28 (m, 2H), 2.27−2.17 (m, 2H). ^{13}C NMR (400 MHz, $CDCl_3$): δ 151.1, 132.4, 128.5, 125.5, 125.2, 124.6, 122.2, 74.9, 33.6, 29.7, 29.4.

AnPy. 9-(4-Bromobutoxy)anthracene (120 mg, 0.36 mmol) and pyridine (1 mL) were dissolved in acetone (25 mL), and the solution was heated to reflux for 24 h under an argon atmosphere (Scheme 2).

Scheme 2. Synthesis of AnPy

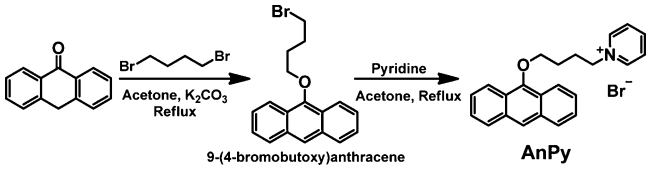

After cooling to room temperature, the mixture was poured into anhydrous diethyl ether (300 mL) with vigorous stirring. The precipitates produced were filtered and washed with diethyl ether. The product was dried overnight under vacuum (yield: 100 mg, 67%). MS: m/z 328.2 ([AnPy − Br]$^+$, calcd for $C_{23}H_{22}NO^+$, 328.2). ^{1}H NMR (400 MHz, D_2O): δ 8.49 (d, 2H), 8.27 (t, 1H), 7.97−7.84 (m, 3H), 7.80−7.61 (m, 4H), 7.38−7.16 (m, 4H), 4.38 (t, 2H), 3.84 (t, 2H), 2.00−1.84 (m, 2H), 1.75−1.59 (m, 2H). ^{13}C NMR (400 MHz, D_2O): δ 149.3, 145.6, 144.0, 132.0, 128.5, 128.2, 126.0, 124.0, 122.8, 121.5, 75.0, 61.5, 27.5, 26.1.

Measurements. *Irradiation.* The solution of the SC4A−AnPy assembly was placed in centrifugal tubes (5 mL) and further irradiated using a 500 W medium-pressure mercury lamp (CEL-M500) under air at room temperature. After irradiation, the UV−vis spectra of the supramolecular assembly were measured at 40 °C to eliminate inaccuracy in the absorption spectra caused by light scattering of particles because the assembly could completely disassemble at this temperature.

UV−vis Spectroscopy. The optical transmittance and absorbance of the aqueous solution were measured in a quartz cell (light path, 10 mm) on a Shimadzu UV-3600 spectrophotometer equipped with a PTC-348WI temperature controller.

Fluorescence Spectroscopy. Steady-state fluorescence spectra were recorded in a conventional quartz cell (light path, 10 mm) on a Varian Cary Eclipse equipped with a Varian Cary single-cell Peltier accessory to control the temperature.

NMR Spectroscopy. ^{1}H NMR spectra were recorded on a Bruker AV400 spectrometer at 25 °C.

TEM Measurement. TEM images were acquired using a Tecnai 20 transmission electron microscope operating at an accelerating voltage of 200 kV. The sample for TEM measurements was prepared by dropping a sample solution onto a copper grid. The grid was then air-dried.

DLS Measurement. Solution samples were examined on a laser light scattering spectrometer (BI-200SM) equipped with a digital correlator (TurboCorr) at 636 nm at a scattering angle of 90°. The hydrodynamic diameter (D_h) was determined by DLS experiments at 25 °C.

Zeta (ζ) Potential Measurement. Zeta potential values were determined at 25 °C on a Brookhaven ZetaPALS (Brookhaven Instrument, USA). The instrument utilizes phase analysis light scattering to provide an average over multiple particles. Doubly distilled water was used as the background electrolyte for ζ potential measurements.

ASSOCIATED CONTENT

Supporting Information

Characterization of compound AnPy, Job plot, additional optical transmittance and UV−vis curves, ζ potential, and photodecomposition product analysis are provided. This material is available free of charge via the Internet at http://pubs.acs.org.

AUTHOR INFORMATION

Corresponding Author

*yuliu@nankai.edu.cn

Notes

The authors declare no competing financial interest.

ACKNOWLEDGMENTS

We thank the "973" Program (no. 2011CB932502) and NNSFC (nos. 91227107, 21432004, and 21472100) for financial support.

REFERENCES

(1) (a) Burnworth, M.; Tang, L.; Kumpfer, J. R.; Duncan, A. J.; Beyer, F. L.; Fiore, G. L.; Rowan, S. J.; Weder, C. *Nature* **2011**, *472*, 334−337. (b) Ma, X.; Tian, H. *Chem. Soc. Rev.* **2010**, *39*, 70−80. (c) Pellizzaro, M. L.; Houton, K. A.; Wilson, A. *Chem. Sci.* **2013**, *4*, 1825−1829.

(2) (a) Huang, Y.; Dong, R.; Zhu, X.; Yan, D. *Soft Matter* **2014**, *10*, 6121−6138. (b) Zhang, Q.; Qu, D.-H.; Ma, X.; Tian, H. *Chem. Commun.* **2013**, *49*, 9800−9802. (c) Wang, Y.; Xu, H.; Zhang, X. *Adv. Mater.* **2009**, *21*, 2849−2864.

(3) Itoh, Y.; Horiuchi, S.; Yamamoto, K. *Photochem. Photobiol. Sci.* **2005**, *4*, 835−839.

(4) Itoh, Y.; Yamamoto, K.; Shirai, H. *Chem. Lett.* **2003**, *32*, 8−9.

(5) Detty, M. R.; Gibson, S. L.; Wagner, S. J. *J. Med. Chem.* **2004**, *47*, 3897−3915.

(6) (a) Kloxin, A. M.; Kasko, A. M.; Salinas, C. N.; Anseth, K. S. *Science* **2009**, *324*, 59−63. (b) de la Orden, M. U.; Montes, J. M.; Urreaga, J. M.; Bento, A.; Ribeir, M. R.; Perez, E.; Cerrada, M. L. *Polym. Degrad. Stab.* **2015**, *111*, 78−88. (c) Sun, L.; Yang, Y.; Dong, C. M.; Wei, Y. *Small* **2011**, *7*, 401−406. (d) Chen, C. C.; Ma, W. H.; Zhao, J. C. *Chem. Soc. Rev.* **2010**, *39*, 4206−4219. (e) Zhao, W.; Ma,

DOI: 10.1021/jacs.5b01566
J. Am. Chem. Soc. 2015, 137, 4543−4549

W. H.; Chen, C. C.; Zhao, J. C.; Shuai, Z. G. *J. Am. Chem. Soc.* **2004**, *126*, 4782−4783.
(7) (a) Estroff, L. A.; Hamilton, A. D. *Chem. Rev.* **2004**, *104*, 1201−1217. (b) Buerkle, L. E.; Rowan, S. J. *Chem. Soc. Rev.* **2012**, *41*, 6089−6102. (c) Wang, Y.-X.; Guo, D.-S.; Cao, Y.; Liu, Y. *RSC Adv.* **2013**, *3*, 8058−8063.
(8) (a) Liu, Y.; Yu, C. Y.; Jin, H. B.; Jiang, B. B.; Zhu, X. Y.; Zhou, Y. F.; Lv, Z. Y.; Yan, D. Y. *J. Am. Chem. Soc.* **2013**, *135*, 4765−4770. (b) Xu, J.; Chen, Y.; Wu, D.; Wu, L.; Tung, C.; Yang, Q. *Angew. Chem., Int. Ed.* **2013**, *52*, 9738−9742. (c) Wang, Y. P.; Ma, N.; Wang, Z. Q.; Zhang, X. *Angew. Chem., Int. Ed.* **2007**, *46*, 2823−2826. (d) Yu, G.; Han, C.; Zhang, Z.; Chen, J.; Yan, X.; Zheng, B.; Liu, S.; Huang, F. *J. Am. Chem. Soc.* **2012**, *134*, 8711−8717. (e) Yan, X.; Xu, J.; Cook, T. R.; Huang, F.; Yang, Q.; Tung, C.; Stang, P. J. *Proc. Natl. Acad. Sci. U. S. A.* **2014**, *111*, 8717−8722. (f) Liao, X.; Chen, G.; Liu, X.; Chen, W.; Chen, F.; Jiang, M. *Angew. Chem., Int. Ed.* **2010**, *49*, 4409−4413.
(9) (a) Guo, D.-S.; Liu, Y. *Chem. Soc. Rev.* **2012**, *41*, 5907−5921. (b) Kim, K.; Selvapalam, N.; Ko, Y. H.; Park, K. M.; Kim, D.; Kim, J. *Chem. Soc. Rev.* **2007**, *36*, 267−279. (c) Harada, A.; Takashima, Y.; Yamaguchi, H. *Chem. Soc. Rev.* **2009**, *38*, 875−882.
(10) (a) Guo, D.-S.; Zhang, T.-X.; Wang, Y.-X.; Liu, Y. *Chem. Commun.* **2013**, *49*, 6779−6781. (b) Shinkai, S.; Araki, K.; Matsuda, T.; Nishiyama, N.; Ikeda, H.; Takasu, I.; Iwamoto, M. *J. Am. Chem. Soc.* **1990**, *112*, 9053−9058. (c) Liu, Y.; Guo, D.-S.; Zhang, H.-Y.; Ma, Y.-H.; Yang, E.-C. *J. Phys. Chem. B* **2006**, *110*, 3428−3434.
(11) (a) Perret, F.; Lazar, A. N.; Coleman, A. W. *Chem. Commun.* **2006**, 2425−2438. (b) Perret, F.; Coleman, A. W. *Chem. Commun.* **2011**, *47*, 7303−7319. (c) Wang, Y.-X.; Guo, D.-S.; Duan, Y.-C.; Wang, Y.-J.; Liu, Y. *Sci. Rep.* **2015**, *5*, 9019.
(12) (a) Guo, D.-S.; Liu, Y. *Acc. Chem. Res.* **2014**, *47*, 1925−1934. (b) Guo, D.-S.; Wang, K.; Wang, Y.-X.; Liu, Y. *J. Am. Chem. Soc.* **2012**, *134*, 10244−10250. (c) Cao, Y.; Wang, Y.-X.; Guo, D.-S.; Liu, Y. *Sci. China Chem.* **2014**, *57*, 371−378.
(13) (a) Xu, J.-F.; Chen, Y.-Z.; Wu, L.-Z.; Tung, C.-H.; Yang, Q.-Z. *Org. Lett.* **2013**, *15*, 6148−6151. (b) Wang, Q.; Yang, C.; Ke, C.; Fukuhara, G.; Mori, T.; Liu, Y.; Inoue, Y. *Chem. Commun.* **2011**, *47*, 6849−6851. (c) Connal, L. A.; Vestberg, R.; Hawker, C. J.; Qiao, G. G. *Adv. Funct. Mater.* **2008**, *18*, 3315−3322.
(14) (a) Song, B.; Wang, G.; Tan, M.; Yuan, J. *J. Am. Chem. Soc.* **2006**, *128*, 13442−13450. (b) Umezawa, N.; Tanaka, K.; Urano, Y.; Kikuchi, K.; Higuchi, T.; Nagano, T. *Angew. Chem., Int. Ed.* **1999**, *38*, 2899−2901. (c) Tanaka, K.; Miura, T.; Umezawa, N.; Urano, Y.; Kikuchi, K.; Higuchi, T.; Nagano, T. *J. Am. Chem. Soc.* **2001**, *123*, 2530−2536. (d) Arian, D.; Kovbasyuk, L.; Mokhir, A. *J. Am. Chem. Soc.* **2011**, *133*, 3972−3980.
(15) Yan, Q.; Hu, J.; Zhou, R.; Ju, Y.; Yin, Y.; Yuan, J. *Chem. Commun.* **2012**, *48*, 1913−1915.
(16) Jiang, B.-P.; Guo, D.-S.; Liu, Y.-C.; Wang, K.-P.; Liu, Y. *ACS Nano* **2014**, *8*, 1609−1618.
(17) Liu, K.; Liu, Y.; Yao, Y.; Yuan, H.; Wang, S.; Wang, Z.; Zhang, X. *Angew. Chem., Int. Ed.* **2013**, *52*, 8285−8289.
(18) Zhang, T.; Sun, S.; Liu, F.; Pang, Y.; Fan, J.; Peng, X. *Phys. Chem. Chem. Phys.* **2011**, *13*, 9789−9795.
(19) Rehm, M.; Frank, M.; Schatz, J. *Tetrahedron Lett.* **2009**, *50*, 93−96.
(20) Lekha, P. K.; Prasad, E. *Chem.—Eur. J.* **2010**, *16*, 3699−3706.
(21) Hu, J.; Wang, P.; Lin, Y.; Zhang, J.; Smith, M.; Pellechia, P. J.; Yang, S.; Song, B.; Wang, Q. *Chem.—Eur. J.* **2014**, *20*, 7603−7607.
(22) Arena, G.; Casnati, A.; Contino, A.; Lombardo, G. G.; Sciotto, D.; Ungaro, R. *Chem.—Eur. J.* **1999**, *5*, 738−744.
(23) Matsumiya, H.; Terazono, Y.; Iki, N.; Miyano, S. *J. Chem. Soc., Perkin Trans. 2* **2002**, 1166−1172.
(24) (a) Guo, D.-S.; Wang, K.; Liu, Y. *J. Inclusion Phenom. Macrocyclic Chem.* **2008**, *62*, 1−21. (b) Chen, Z.; Lohr, A.; Saha-Möller, C. R.; Würthner, F. *Chem. Soc. Rev.* **2009**, *38*, 564−584. (c) Chen, Z.; Stepanenko, V.; Dehm, V.; Prins, P.; Siebbeles, L. D. A.; Seibt, J.; Marquetand, P.; Engel, V.; Würthner, F. *Chem.—Eur. J.* **2007**, *13*, 436−449. (d) Ford, D. M. *J. Am. Chem. Soc.* **2005**, *127*, 16167−16170.
(25) (a) Bowen, E. J. *Discuss. Faraday Soc.* **1953**, *14*, 143−146. (b) Kohtani, S.; Tomohiro, M.; Tokumura, K.; Nakagaki, R. *Appl. Catal., B* **2005**, *58*, 265−272.
(26) (a) Barnett, W. E.; Needham, L. L. *J. Org. Chem.* **1971**, *36*, 4134−4136. (b) Powell, M. F. *J. Org. Chem.* **1987**, *52*, 56−61.
(27) Wang, K.; Guo, D.-S.; Wang, X.; Liu, Y. *ACS Nano* **2011**, *5*, 2880−2894.
(28) (a) Fernández, D. A.; Awruch, J.; Dicelio, L. E. *Photochem. Photobiol.* **1996**, *63*, 784−792. (b) Voskuhl, J.; Kauscher, U.; Gruener, M.; Frisch, H.; Wibbeling, B.; Strassert, C. A.; Ravoo, B. J. *Soft Matter* **2013**, *9*, 2453−2457.
(29) (a) Merkel, P. B.; Kearns, D. R. *J. Am. Chem. Soc.* **1972**, *94*, 1029−1030. (b) Murov, S. L.; Hug, G. L.; Carmichael, I. *Handbook of Photochemistry*; Marcel Dekker, Inc.: New York, 1993; pp 289−293.
(30) (a) Hariharan, M.; Karunakaran, S. C.; Ramaiah, D.; Schulz, I.; Epe, B. *Chem. Commun.* **2010**, *46*, 2064−2066. (b) Li, G.; Graham, A.; Chen, Y.; Dobhal, M. P.; Morgan, J.; Zheng, G.; Kozyrev, A.; Oseroff, A.; Dougherty, T. J.; Pandey, R. K. *J. Med. Chem.* **2003**, *46*, 5349−5359.
(31) Zhao, H.-X.; Guo, D.-S.; Liu, Y. *J. Phys. Chem. B* **2013**, *117*, 1978−1987.

DOI: 10.1021/jacs.5b01566
J. Am. Chem. Soc. 2015, 137, 4543−4549